Drug Design, Development and Therapy

Dovepress
open access to scientific and medical research

Open Access Full Text Article

ORIGINAL RESEARCH

Synergistic Combination Chemotherapy of Lung Cancer: Cisplatin and Doxorubicin Conjugated Prodrug Loaded, Glutathione and pH Sensitive Nanocarriers

This article was published in the following Dove Press journal:
Drug Design, Development and Therapy

Yonglong Jin[1,*]
Yi Wang[2,*]
Xiguang Liu[1]
Jing Zhou[1]
Xintong Wang[1]
Hui Feng[1]
Hong Liu[2]

[1]Department of Radiotherapy, Affiliated Hospital of Qingdao University, Qingdao 266000, People's Republic of China; [2]Department of Radiation Oncology, Qilu Hospital of Shandong University, Jinan 250012, People's Republic of China

*These authors contributed equally to this work

Purpose: Prodrug technology-based combination drug therapy has been exploited as a promising treatment strategy to achieve synergistic lung cancer therapy, reduce drug dose, and decrease side effects. In the present study, we synthesized a pH and glutathione (GSH) sensitive prodrug, cisplatin (CIS) and doxorubicin (DOX) conjugates (CIS-DOXp). CIS-DOXp was loaded by nanocarriers and delivered into the tumor site.

Methods: pH and GSH sensitive CIS-DOX prodrug (CIS-DOXp) was synthesized by conjugating GSH responsive CIS prodrug with pH sensitive DOX prodrug. CIS-DOXp-loaded nanocarriers (CIS-DOXp NC) were prepared using emulsification and solvent evaporation method. The morphology, particle size, polydispersity index (PDI) and zeta potential of nanocarriers were measured. In vitro cytotoxicity of nanocarriers and the corresponding free drugs was examined using the MTT assay. In vivo anti-tumor efficiency and biodistribution behaviors were evaluated on lung cancer mice models.

Results: The size, PDI, zeta potential, CIS loading efficiency, and DOX loading efficiency of CIS-DOXp NC were 128.6 ± 3.2 nm, 0.196 ± 0.021, 15.7 ± 1.7 mV, 92.1 ± 2.1%, and 90.4 ± 1.8%, respectively. The best cell killing ability (the lowest combination index of 0.57) was found at the combination ratio of 1:3 (CIS:DOX, w/w) in the drugs co-loaded formulations, indicating the strongest synergism effect. CIS-DOXp NC showed the best tumor inhibition efficiency (79.9%) in mice with negligible body weight lost.

Conclusion: CIS-DOXp NC could be applied as a promising system for the synergistic chemotherapy of lung cancer.

Keywords: lung cancer, combination therapy, prodrug, pH responsive, GSH responsive

Introduction

Lung cancer is the leading cause of cancer-related death in the United States and worldwide, and this accounts for about 24% of all cancer deaths in USA.[1,2] Poor diagnosis and limited therapeutic therapies have led to mostly evolved advanced-stage lung cancer patients and lower five-year survival rates (only 19%).[3] It is generally known that systemic therapy is the most commonly applied therapeutic regimen for advanced or metastatic lung cancer patients. Whereas, chemotherapy regimens have faced various challenges hindering efficacy, including lack of tumor-targeting, serious toxic effects on healthy tissues, and multidrug resistance.[4,5] Recently, researchers have devoted into new strategies to solve the aforementioned

Correspondence: Hong Liu
Department of Radiation Oncology, Qilu Hospital of Shandong University, No. 107 West Wenhua Road, Jinan, Shandong, People's Republic of China
Email liuhongsdu@163.com

submit your manuscript | www.dovepress.com
DovePress
http://doi.org/10.2147/DDDT.S260253

issues containing prodrug technology-based combination therapy, and novel nanoscale targeting approaches (targeting the tumor microenvironment, such as the acidic pH, high concentration of glutathione, etc).[6–9]

Prodrug technology-based combination drug therapy has been exploited as a promising treatment strategy to achieve synergistic cancer therapy, minimal drug dose, and decreased side effects.[10,11] Prodrug technology-based combination drug therapy consists of at least three types of systems: two independent anticancer prodrugs; one free anticancer drug and another prodrug; and conjugates composed of two different anticancer drugs.[11] In the present study, we synthesized a pH sensitive and glutathione (GSH) sensitive prodrug, cisplatin (CIS) and doxorubicin (DOX) conjugates. CIS is recommended as the first-line therapy for lung cancer by the NCCN guidelines. CIS is a DNA alkylating agent, can bind with genomic DNA and interfere with normal transcription and/or DNA replication, thus triggering toxicity.[12] DOX, a broad-spectrum antitumor chemotherapeutic drug, has been applied in the treatment of a variety of cancers.[13] CIS has been combined with DOX for lung cancer therapy, showing a significant therapeutic effect.[14–16] As is well known that both CIS and DOX are hydrophobic agents, pH and GSH sensitive CIS-DOX prodrug has the similar properties and could be loaded by nanocarriers and delivered into the tumor site.

For stimuli-responsive nanocarriers, anti-cancer agents can be delivered and release at targeting locations to reach ideal therapeutic anticipation. Among the common stimuli-triggered strategies, pH sensitive is the most frequently researched and used in recent cancer therapy fields.[17] Prodrug-based pH sensitive nanoparticles can be achieved by sensitive chemical linkers such as hydrazone bonds, acetal linkage, etc.[18–20] In our study, DOX and CIS were conjugated by the hydrazone bond and GSH sensitive linker. It is known that the GSH concentration in tumor cells is at least two-folds that for normal cells and intracellular GSH in cisplatin-resistant cells is two-folds as high as that in cisplatin-sensitive cells.[21,22] Therefore, nanocarriers that loaded CIS-DOX pH sensitive and GSH sensitive prodrug (CIS-DOXp) were exploited to realize double efficiencies.

Lipid nanocarriers were designed to encapsulate the previously prepared CIS-DOXp. The drug ratios of CIS to DOX were evaluated by combination index and the physicochemical propriety of CIS-DOXp loaded nanocarriers (CIS-DOXp NC). Release studies were applied in GSH contained medium at different pH values. In vitro cytotoxicity of CIS-DOXp NC was evaluated for lung cancer and drug-resistance lung cancer cells. Tumor-bearing mice were utilized to determine the in vivo anticancer efficiency and systemic toxicity drug forms.

Materials and Methods

Materials

CIS, DOX, 1-(3-Dimethylaminopropyl)-3-ethylcarbodiimide hydrochloride (EDC), glyceryl monostearate (GMS), and soya lecithin (SL) were obtained from Sigma-Aldrich China (Shanghai, China). Compound 1 (Figure 1) was purchased from TCI China. RPMI Medium 1640, fetal bovine serum (FBS) and 3-(4,5-dimethyl-2-thiazolyl)-2,5-diphenyl-2-H-tetrazolium bromide (MTT) were purchased from Invitrogen Corporation (Carlsbad, CA).

Synthesis of pH and GSH Sensitive CIS-DOX Prodrug

GSH and pH sensitive CIS-DOX prodrug (CIS-DOXp) was synthesized by conjugating GSH sensitive CIS prodrug with pH sensitive DOX prodrug (Figure 1).

Firstly, GSH sensitive CIS prodrug was synthesized.[23,24] CIS was treated with hydrogen peroxide to obtain $Pt(NH_3)_2Cl_2(OH)_2$. $Pt(NH_3)_2Cl_2(OH)_2$ (1 equivalent) was reacted with Compound 1 (2.2 equivalents) overnight to form $Pt(NH_3)_2Cl_2(OCOC_6H_{12}COOH)_2$.

Secondly, pH sensitive DOX prodrug was synthesized.[20,25] Adipohydrazide (1 equivalent) and EDC (2 equivalents) were reacted in water solution at room temperature for 6 h. DOX (1.2 equivalents) was then added and reacted under acid conditions overnight to form DOX prodrug.

Finally, DOX prodrug (2 equivalents) was activated by EDC (3 equivalents) and $Pt(NH_3)_2Cl_2(OCOC_6H_{12}COOH)_2$ (1 equivalent) was added and reacted overnight to get CIS-DOXp. The structure of CIS-DOXp was determined by LC-MS and ^1H NMR.

Construction of CIS-DOXp-Loaded Nanocarriers

CIS-DOXp NC was prepared using emulsification and the solvent evaporation method.[26,27] CIS-DOXp (20 mg), GMS (50 mg) and soya lecithin (100 mg) were dissolved in chloroform (10 mL) to produce an oil phase. The oil phase was added to an aqueous phase containing Tween 80 (1.5%) and homogenized (10,000 rpm for 3 min) to get an emulsion. The emulsion was sonicated for 5 min to obtain CIS-DOXp NC.

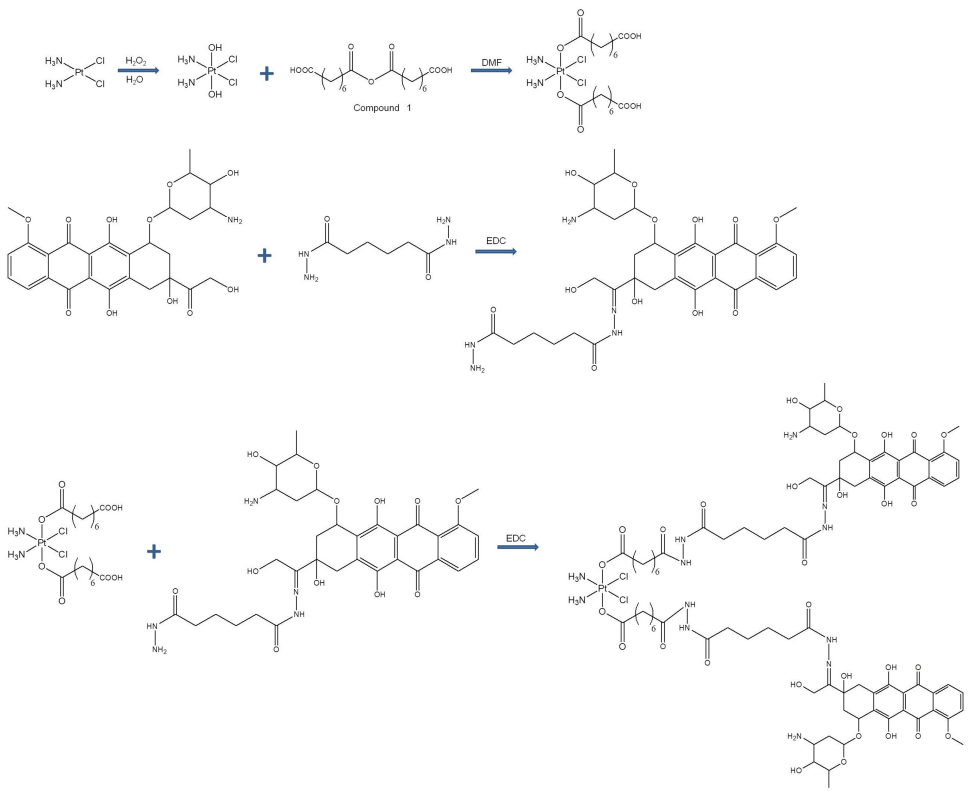

Figure 1 Synthesis of pH and GSH sensitive CIS-DOX prodrug (CIS-DOXp): CIS-DOXp was synthesized by conjugating GSH sensitive CIS prodrug with pH sensitive DOX prodrug.

Non-prodrug contained nanocarriers were prepared using the same method using CIS (5 mg) and DOX (15 mg) instead of CIS-DOXp (20 mg), namely CIS/DOX NC; using CIS (10 mg) instead of CIS-DOXp (20 mg), namely CIS NC; using DOX (30 mg) instead of CIS-DOXp (20 mg), namely DOX NC. Blank nanocarriers (NC) were prepared using the same method without the presence of any drug.

Morphology, Particle Size, and Zeta Potential

The morphology of the CIS-DOXp NC was visualized by transmission electron microscopy (TEM, JEOL 100CX, Tokyo, Japan).[28] Particle size, polydispersity index (PDI) and Zeta potential (ζ) of nanocarriers were measured using a Malvern Zetasizer Nano-ZS (Malvern Instruments Ltd, Worcestershire, England) at room temperature.

Colloidal and Serum Stability

The colloidal stability of nanocarriers was determined by measuring the particle size over a 30-day period at two storage conditions: 4°C or 25°C.[29] The serum stability of nanocarriers was performed in 50% FBS and incubated at 37°C for various time periods, monitoring the particle size changes.

Drug Loading and Drug Release in vitro

To determine the drug loading, nanocarriers ethanol solution (1 mL) was centrifuged at 15, 000 rpm for 10 min and dissolved in 10 mL KOH (1 M) for 2 h. Then, HCl (10 mL, 1.0 M) was added for neutralizing.[30] The suspension was centrifuged at 15, 000 rpm for 10 min, followed by collecting and the upper clear solutions. The drug loading efficiency (LE) and drug loading content (LC) of CIS and DOX were determined by UV-vis spectrometer and ICP-OES. LE and LC were calculated according to the following formulas:

$$\mathrm{LE}\,(\%) = (\text{weight of loaded drug}/\text{weight of feeding drug}) \times 100$$

$$\mathrm{LC}(\%) = \left(\begin{array}{l}\text{weight of loaded drug}/\\ \textit{weight of drugs loaded nanocarriers}\end{array}\right) \times 100$$

The release of drugs from nanocarriers was evaluated by centrifuging (15, 000 rpm for 10 min) the nanocarriers ethanol solution (0.5 mL).[31] The resulting solid was

dispersed in PBS (15 mL, pH 7.4) with or without GSH (10 mM) at different pH values (pH 7.4 or 5.0). The suspensions were equally distributed to 15 vials (1 mL each) and then incubated at 37°C. One vial of each group was taken out at determined time points and centrifuged (15, 000 rpm for 10 min). The supernatants were taken out and the amount of CIS and DOX was determined by the same method above.

Cells and Animals

Human non-small cell lung cancer cell line: A549 cells were purchased from American Type Culture Collection (ATCC, Manassas, VA). CIS resistance lung cancer cell line: A549/CIS cells were provided by Shanghai Ai Research Biological Technology Co., Ltd (Shanghai, China). Cells were cultured in RPMI Medium 1640 supplemented with 10% (v/v) FBS and 1% (v/v) penicillin–streptomycin at 37°C in an atmosphere of 5% CO_2.

Female BABL/c mice (20 ± 2 g) were provided by Shandong University Laboratory Animal Center (Ji'nan, China) and the mice are maintained and treated in compliance with the policy of the National Institutes of Health guide for the care and use of Laboratory animals and the protocols were approved by the Animal Use and Care Committee of Qilu Hospital of Shandong University.

In vitro Cytotoxicity

The in vitro cytotoxicity of nanocarriers and the corresponding free drugs was examined using the MTT assay.[32] A549 cells or A549/CIS cells were seeded in 96-well plates (1000 cells per well) and incubated for 12 h and exposed to CIS-DOXp NC, CIS-DOX NC, CIS NC, DOX NC, and free CIS-DOX. After 48 h, MTT (5 mg/mL, 15 mL) dissolved in phosphate-buffered saline (PBS) was added to each well and incubated for another 3 h, and DMSO (15 mL) was added to each well. The absorbance at 570 nm was measured.

In vitro Synergistic Effect

Synergistic drug combinations are usually evaluated by median-effect analysis.[33] The median-effect method assesses the drug–drug interaction by a term called the "combination index" (CI), which is based on the concentration–response relationship. CI was used to evaluate synergy between CIS and DOX combination against A549/CIS cells, which was performed by CalcuSyn software 1.0. Values of CI < 1, = 1, and > 1 indicate synergy, additivity, and antagonism, respectively.

In vivo Antitumor Effect

A549/CIS cells (100 μL, contained 1×10^6 cells) were subcutaneous injected to the right flank of mice to obtain lung tumor-bearing models.[34] When the mean tumor volume reached approximately 100 mm^3, tumor-bearing mice were randomly divided into seven treatment groups (eight mice per group), receiving every three days via intravenous tail injection until day 18 with (1) CIS-DOXp NC (CIS 5 mg, DOX 15 mg), (2) CIS-DOX NC (CIS 5 mg, DOX 15 mg), (3) CIS NC (CIS 10 mg), (4) DOX NC (DOX 30 mg), (5) free CIS-DOX (CIS 5 mg, DOX 15 mg), (6) NC, and (7) normal saline (NS). Tumor volume and body weight were measured before each injection. Tumor volume (TV) was calculated by the following formula:

$$TV = \left(\text{longest diameter} \times \text{shortest diameter}^2\right)/2$$

The tumor inhibition rates were calculated according to the tumor volume changes and the tumor images were captured at the end of study.

In vivo Biodistribution

The above-obtained tumor-bearing mice were randomly divided into three treatment groups (eight mice per group), receiving (1) CIS-DOXp NC (CIS 5 mg, DOX 15 mg), (2) CIS-DOX NC (CIS 5 mg, DOX 15 mg), and (3) free CIS-DOX.[35] Tumor, heart, liver, spleen, lung, and kidney samples were excised and collected at 2 and 12 h after administration. The tissues were homogenized in lysis buffer, mixed with methanol, and then centrifuged for 30 min. The amount of CIS and DOX was determined by the same method in "Drug loading and drug release in vitro" section.

Statistical Analysis

Data are presented as means ±standard deviation (SD). Statistical analysis was performed by Student's *t*-test between two groups, and one-way analysis of variance (ANOVA) among multiple groups. *P < 0.05 was considered statistically significant.

Results

Characterization of CIS-DOXp

CIS-DOXp prodrug was characterized using LC-MS and ^{1}H NMR. LC-MS (ES+): m/z calculated for C82H108Cl2N12O30Pt: [M + H]+ 2005.6147, found 2005.6325. ^{1}H NMR (400 MHz, DMSO-d6): δ 1.29, 1.57, 2.01 and 2.23 belong to CIS prodrug; δ 2.18, 2.82,

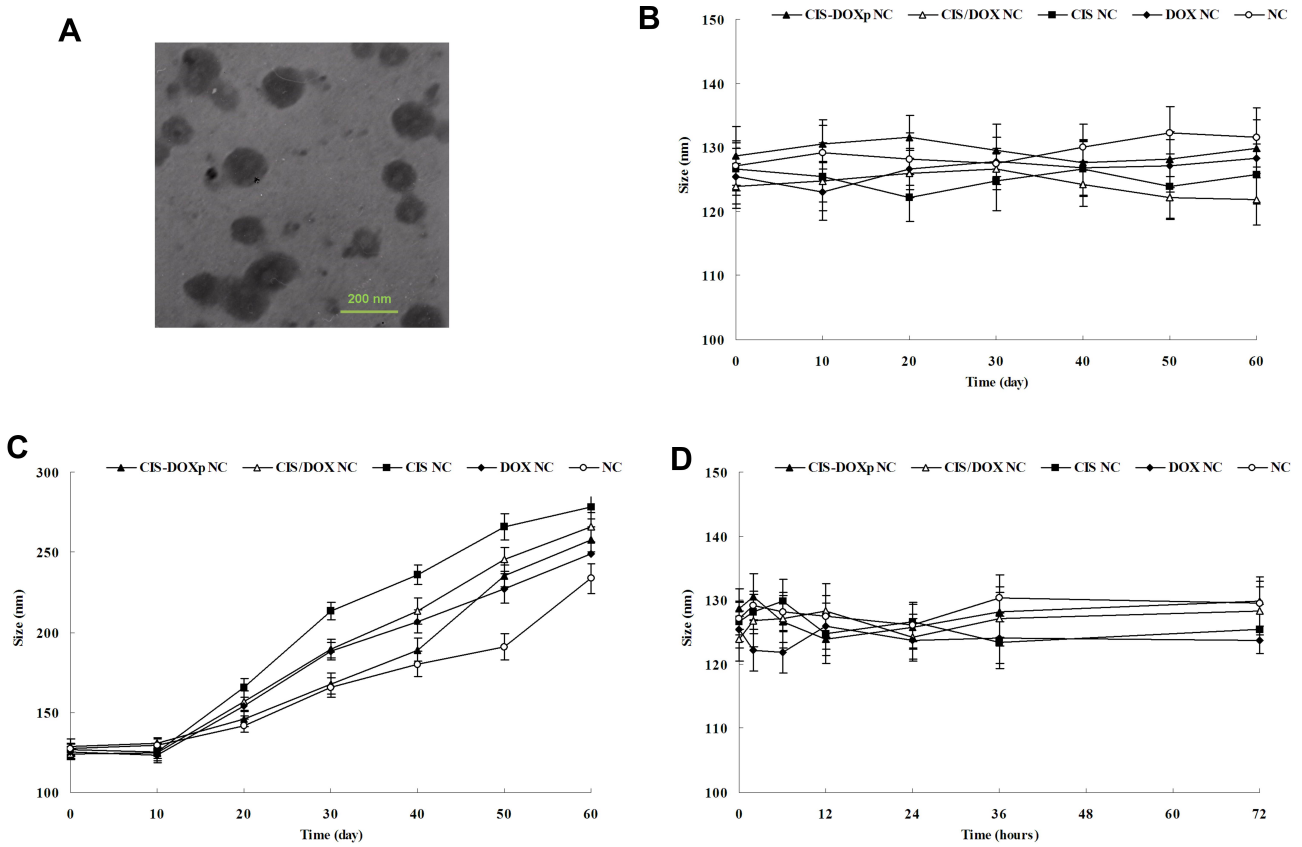

Figure 2 The morphology of the CIS-DOXp NC (**A**); the average diameters of nanocarriers monitored at 4°C for 60 days (**B**); the average diameters of nanocarriers monitored at 25°C for 60 days (Figure 2 (**C**). The serum stability of nanocarriers performed for 72 h (**D**). Data presented as mean ±SD, n=8.

3.73, 4.96, 5.01, 7.36 and 8.03 belong to DOX prodrug. The compound yield was 62.3%.

Characterization of CIS-DOXp-Loaded Nanocarriers

The morphology of the CIS-DOXp NC was mostly spherical and uniform (Figure 2A). The size, PDI, zeta potential, CIS LE, and DOX LE were 128.6 ± 3.2 nm, 0.196 ± 0.021, 15.7 ± 1.7 mV, 92.1 ± 2.1%, and 90.4 ± 1.8%, respectively (Table 1). Other nanocarriers showed similar data on these physicochemical properties, indicating the well-designed nature of the systems.

Colloidal and Serum Stability

The colloidal stability was determined by monitoring the change in particle size during storage time. The average diameters of nanocarriers were stable when stored at 4°C for 60 days (Figure 2B), in contrast, a remarkably increase of size was exhibited under storage condition of 25°C from day 20 (Figure 2C). The serum stability of nanocarriers

Table 1 Characterization of Nanocarriers (Mean ± SD, n=3)

Nanocarriers	Particle Size (nm)	PDI	ζ (mV)	LE (%)		LC (%)	
				CIS	DOX	CIS	DOX
CIS-DOXp NC	128.6 ± 3.2	0.196 ± 0.021	15.7 ± 1.7	92.1 ± 2.1	90.4 ± 1.8	5.6 ± 0.6	15.3 ± 1.1
CIS/DOX NC	123.9 ± 4.1	0.202 ± 0.027	13.9 ± 1.9	91.2 ± 2.2	92.5 ± 2.4	5.1 ± 0.5	16.3 ± 0.9
CIS NC	126.7 ± 3.0	0.187 ± 0.019	14.1 ± 1.6	90.5 ± 2.3	/	5.3 ± 0.7	/
DOX NC	125.5 ± 2.9	0.168 ± 0.015	15.5 ± 1.5	/	91.9 ± 2.1	/	14.7 ± 1.2
NC	127.1 ± 2.6	0.155 ± 0.018	14.4 ± 1.3	/	/	/	/

was performed for 72 h (Figure 2D). Sizes of nanocarriers remained unchanged over the test period, indicating the good protect ability of the systems from being degraded by the nuclease in the plasma in the administration period.

Drug Release in vitro

CIS-DOXp NC showed different release behaviors in PBS (pH 7.4) with or without the presence of GSH. However, CIS-DOX NC exhibited similar release patterns in both conditions (Figure 3). CIS-DOXp NC and CIS-DOX NC illustrated different release profiles at pH 7.4 or 5.0. More drugs were released form CIS-DOXp NC in pH 5.0 than pH 7.4, but CIS-DOX NC showed no difference between these two pH values (Figure 3).

In vitro Cytotoxicity

Cytotoxic effects of CIS-DOXp NC, CIS-DOX NC and free CIS-DOX were different when evaluated on A549 cells or A549/CIS cells. A549 cells were more prominently affected by free CIS-DOX when compared with A549/CIS cells, which attributed to the drug-resistance effect of the latter (Figure 4). CIS-DOXp NC showed slight higher cytotoxicity on A549 cells compared to CIS-DOX NC and free CIS-DOX. However, on A549/CIS cells, significant cell growth inhibition efficacy of CIS-DOXp NC was found than that of CIS-DOX NC ($P < 0.05$); CIS-DOX NC exhibited remarkable higher cytotoxicity than CIS NC, DOX NC, and free CIS-DOX ($P < 0.05$).

In vitro Synergistic Effect

In the above section, CIS-DOX NC showed significantly increased cytotoxicity compared with single drug-loaded CIS NC and DOX NC. The A549/CIS cells may have some resistance effect to CIS, so with the increase of DOX amount, the CI values showed obviously reduction (Table 2). The best cell killing ability (the lowest combination index of 0.57) was

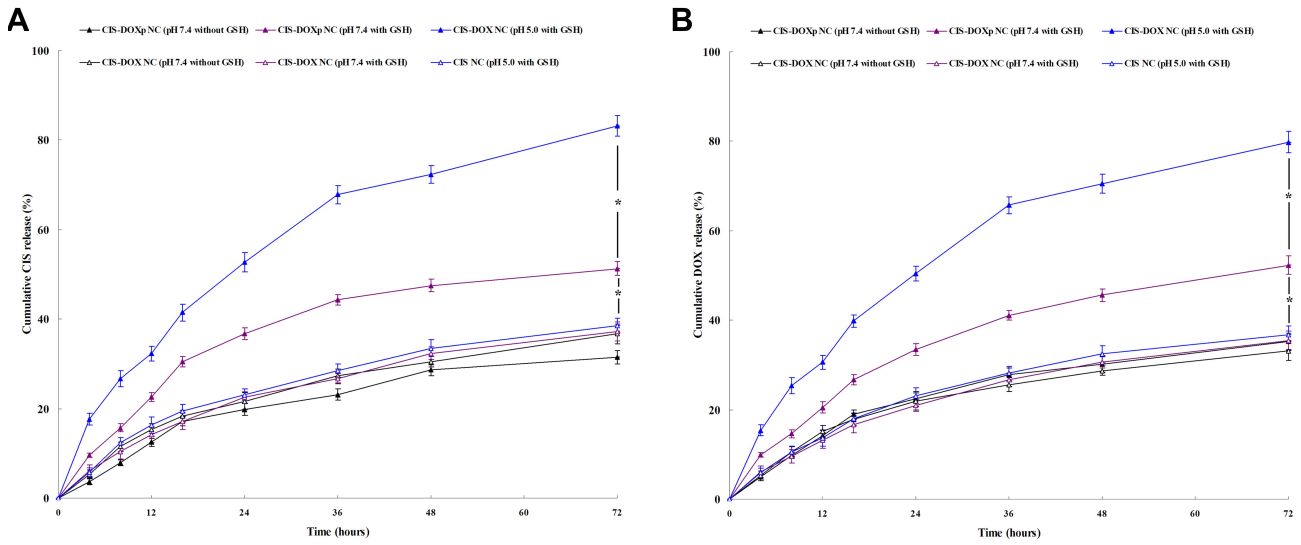

Figure 3 CIS (**A**) and DOX (**B**) release at different pH (7.4 or 5.0) in the medium with or without GSH. Data presented as mean ±SD, n=8, *P < 0.05.

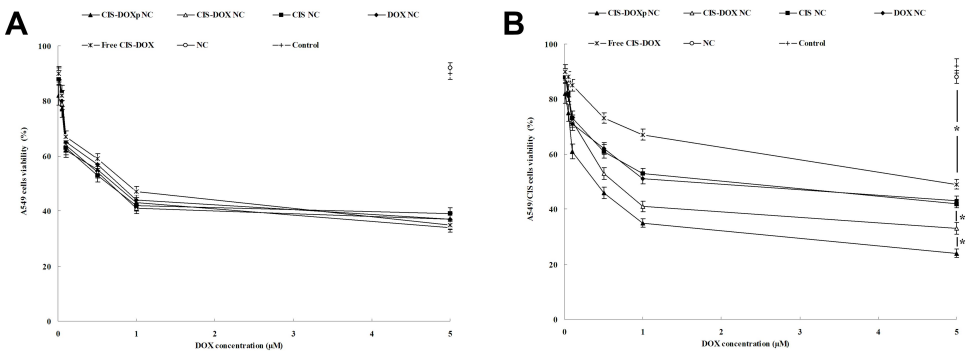

Figure 4 Cytotoxic effects evaluated on A549 cells (**A**) or A549/CIS cells (**B**) by MTT assay. Data presented as mean ±SD, n=8, *P < 0.05.

Table 2 CI Values of Nanocarriers (Mean ± SD, n=3)

Nanocarriers	CIS/DOX (w/w)	IC_{50} (ng/mL)	CI_{50}
CIS NC	–	41.3	–
DOX NC	–	96.1	–
CIS/DOX NC	5:1	49.6/9.9	1.30
	4:1	37.5/9.4	1.01
	3:1	30.4/10.1	0.84
	2:1	27.6/13.8	0.81
	1:1	21.4/21.4	0.74
	1:2	182/36.4	0.82
	1:3	10.3/30.9	0.57
	1:4	13.2/52.8	0.87
	1:5	14.1/70.5	1.08

found at the combination ratio of 1:3 (CIS:DOX, w/w) in the drugs co-loaded formulations, indicating the strongest synergism effect. So this ratio was employed as the amount of drugs in the preparation process.

In vivo Antitumor Effect

Significant in vivo tumor growth inhibition efficiency was achieved by drugs loaded nanocarriers and free drugs groups in comparison with NS and NC groups ($P < 0.05$) (Figure 5A). The tumor images also presented similar results (Figure 5B). The tumor volumes of mice treated with CIS-DOXp NC and CIS-DOX NC were more prominently inhibited than free CIS-DOX group, and the best tumor inhibition efficiency was achieved by CIS-DOXp NC group (79.9 ± 3.5%, Table 3). The body weights of nanocarriers treated mice were steady during the study period.

In vivo Biodistribution

Nanocarriers groups distributed relatively higher in tumor, lower in heart and spleen, and relatively high in liver when compared with free CIS-DOX group (Figure 6). At 2 h, the drug accumulation of free CIS-DOX group was higher than 12 h, which may due to the gradual degradation and metabolism in vivo. On the contrary, the biodistribution of nanocarriers increased at 12 h compared with 2 h, suggesting the long-acting ability of the systems.

Discussion

The tumor microenvironment (TME) is known to encompass unique physicochemical properties that are significantly different from those of the normal tissues. One of the main highlights is generally accepted to be the elevated oxidative stress resulting from the overproduction of reactive oxygen species (ROS) by hypoxic conditions in various TME-associated cells;[36] and another is the acidic TME, which is a consequence of accelerated glycolysis and/or oxidative phosphorylation that provide energy and chemical intermediates for cancer cell proliferation.[36] The nanocarriers prepared in this study contained GSH and pH sensitive prodrug. The GSH sensitive prodrug-based nanocarriers have been designed by researchers and gained excellent anticancer effect.[37–39] pH sensitive prodrugs have also been utilized to deliver more drugs to the acidic tumor site.[40–42] This research combined the GSH and pH sensitive property to one system. The GSH sensitive property of the nanocarriers was evaluated in PBS with or without the presence of GSH to resemble the difference of cellular environment between tumor cells and normal cells.

Release behaviors of drugs loaded in GSH sensitive nanosystems were developed by researchers.[43–45] Hadipour

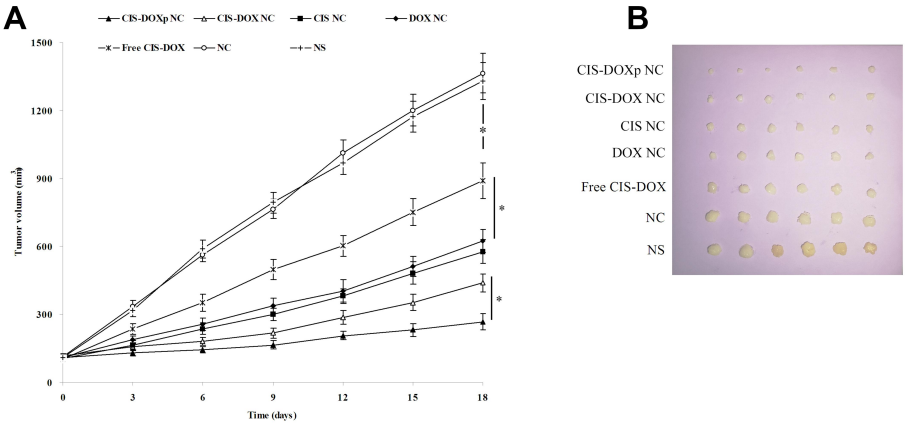

Figure 5 Significant In vivo tumor growth inhibition efficiency: tumor volume curves (**A**), and tumor images (**B**). Data presented as mean ±SD, n=8, *P < 0.05.

Table 3 Tumor Inhibition Efficiency of Nanocarriers (Mean ± SD, n=3)

Nanocarriers	Tumor Inhibition Efficiency (%)
CIS-DOXp NC	79.9 ± 3.5
CIS/DOX NC	70.0 ± 2.8
CIS NC	56.6 ± 2.1
DOX NC	53.1 ± 2.3
Free CIS-DOX	33.1 ± 1.8

Moghaddam and colleagues produced glutathione-sensitive nanoparticles for controlled drug delivery.[43] The redox responsive particles can release drugs approximately up to 60% in the presence of 10 mM of GSH, while drug release from PBS without GSH was about 15%. Similar results were got by the present study that drug release from CIS-DOXp NC was more sufficient in PBS with than without GSH. pH responsive platforms also showed faster and more release when in acidic pH surroundings.[46] In the release section, CIS-DOXp NC released faster and more in pH 5.0 than pH 7.4, which is in accordance with the findings of Poudel and Oladipo et al.[47,48]

The use of multiple therapeutic agents in combination has become the primary strategy to treat drug-resistant cancers.[49] There have been several nano-sized vehicles designed for combination drug delivery in cancer chemotherapy.[11,50,51] Wang et al developed a RGD peptide-modified, CIS and paclitaxel co-loaded lipid-polymer nanoparticles for the enhanced lung cancer therapy, which achieved synergistic tumor cells inhibition ability.[25] Docetaxel and resveratrol co-encapsulated nanocarriers have been prepared by Song and colleagues and exhibited significant synergistic effects.[52] In our study, cytotoxic effects of CIS-DOXp NC evaluated on A549/CIS cells illustrated a strong synergism effect according to the term CI introduced by Chou and Talalay in 1984 for quantification of synergism or antagonism for two drugs.[53]

In tumor tissues, the formation of leaky vessels and pores (100 nm to 2 μm in diameter) and the poor lymphatic system offers great opportunity to treat cancer, which is known as enhanced permeability and retention (EPR) effect.[54] So the nano-sized carriers could facilitate the delivery of drugs to the tumor site.[55] Hong et al argued that nanocarriers near 100 nm in diameter tend to represent an optimal range for leveraging the EPR effect and minimizing clearance.[56] This is in line with our results that CIS-DOXp NC showed a size of 128.6 ± 3.2 nm. The adsorption of proteins on the nanocarriers could cause aggregation, thus leading to an increase in particle size.[57] Also, the storage stability of nanocarriers was important as disruption of the nanoparticles in the drug delivery system may affect its therapeutic potential.[58] Sizes of nanocarriers remained unchanged under 4°C and over the test period in serum storage in this research, indicating the high storage stability and good protection ability of the systems from being degraded by the nuclease in the plasma in the administration period. These advantages enable the

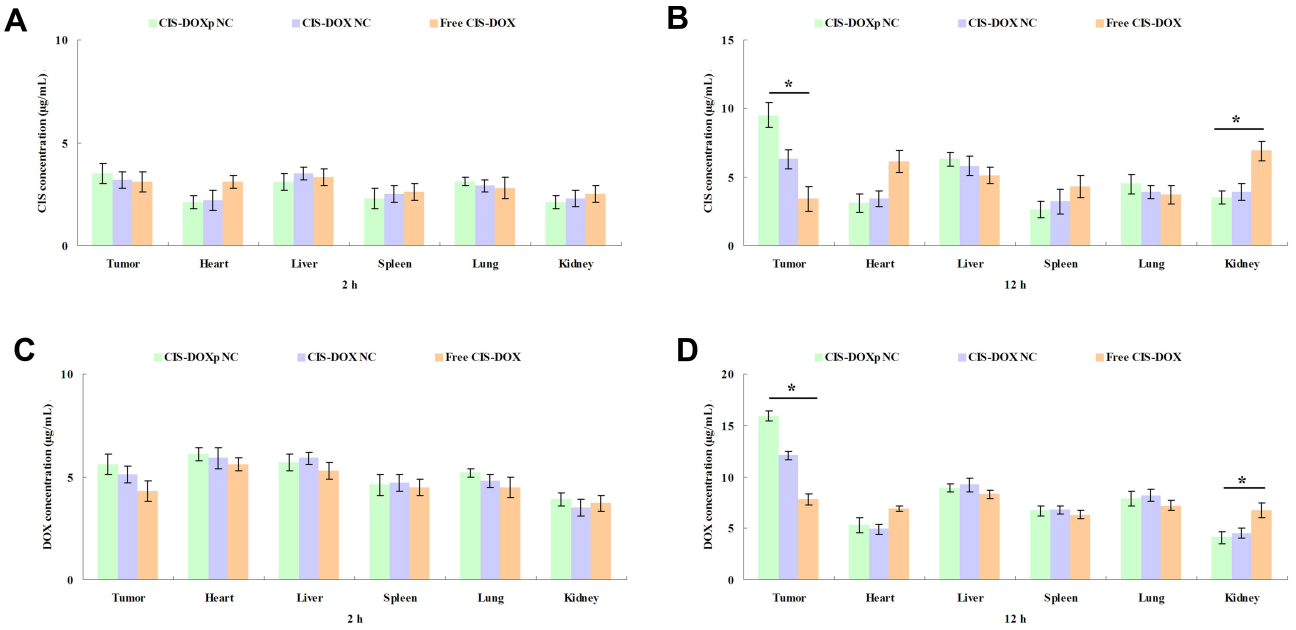

Figure 6 In vivo CIS (**A** and **B**) and DOX (**C** and **D**) biodistribution in tumors and other tissues at 2 (**A** and **C**) and 12 h (**B** and **D**). Data presented as mean ±SD, n=8, *P < 0.05.

system to make use of the EPR effect, so as to achieve an enhanced anti-tumor effect and reduce systemic toxicity. In vivo experiments in this paper have shown remarkable anti-tumor effect and low systemic toxicity. Combined with the system characteristics of combined drug use and double sensitivity, the effectiveness and tolerability of the nano-platform were further illustrated.

Conclusion

In summary, GSH and pH sensitive CIS-DOX prodrug (CIS-DOXp) were synthesized. CIS-DOXp loaded nano-carriers (CIS-DOXp NC) were prepared. CIS-DOXp NC exhibited remarkable cytotoxicity and strong synergism effect. CIS-DOXp NC achieved the best tumor inhibition efficiency in mice with negligible body weight lost, which could be applied as a promising system for the synergistic combination chemotherapy of lung cancer.

Acknowledgments

This research was supported by the Doctoral Foundation of Affiliated Hospital of Qingdao University (No. 111506), the Natural Science Foundation of Shandong Province (ZR2019BH083) and the Youth Scientific Research Foundation of Affiliated Hospital of Qingdao University.

Yonglong Jin and Yi Wang are the co-first authors who contributed equally to this research.

Disclosure

The authors do not have any conflict of interest to declare.

References

1. Siegel RL, Miller KD, Jemal A. Cancer statistics, 2019. *CA Cancer J Clin*. 2019;69(1):7–34. doi:10.3322/caac.21551
2. Torre LA, Siegel RL, Ward EM, Jemal A. Global cancer incidence and mortality rates and trends–an update. *Cancer Epidemiol Biomarkers Prev*. 2016;25(1):16–27. doi:10.1158/1055-9965.EPI-15-0578
3. Jemal A, Bray F, Center MM, Ferlay J, Ward E, Forman D. Global cancer statistics. *CA Cancer J Clin*. 2011;61(2):69–90.
4. Peer D, Karp JM, Hong S, Farokhzad OC, Margalit R, Langer R. Nanocarriers as an emerging platform for cancer therapy. *Nat Nanotechnol*. 2007;2(12):751–760. doi:10.1038/nnano.2007.387
5. He Y, Su Z, Xue L, Xu H, Zhang C. Co-delivery of erlotinib and doxorubicin by pH-sensitive charge conversion nanocarrier for synergistic therapy. *J Control Release*. 2016;10(229):80–92. doi:10.1016/j.jconrel.2016.03.001
6. Dhar S, Gu FX, Langer R, Farokhzad OC, Lippard SJ. Targeted delivery of cisplatin to prostate cancer cells by aptamer functionalized Pt(IV) prodrug-PLGA-PEG nanoparticles. *Proc Natl Acad Sci U S A*. 2008;105(45):17356–17361. doi:10.1073/pnas.0809154105
7. Mi Y, Zhao J, Feng SS. Targeted co-delivery of docetaxel, cisplatin and herceptin by vitamin E TPGS-cisplatin prodrug nanoparticles for multimodality treatment of cancer. *J Control Release*. 2013;169(3):185–192. doi:10.1016/j.jconrel.2013.01.035
8. Ma B, Zhuang W, Wang Y, Luo R, Wang Y. pH-sensitive doxorubicin-conjugated prodrug micelles with charge-conversion for cancer therapy. *Acta Biomater*. 2018;1(70):186–196. doi:10.1016/j.actbio.2018.02.008
9. Huo Q, Liang Y, Lu W, et al. Integrated metalloproteinase, pH and glutathione responsive prodrug-based nanomedicine for efficient target chemotherapy. *J Biomed Nanotechnol*. 2019;15(8):1673–1687. doi:10.1166/jbn.2019.2801
10. Ling L, Ismail M, Shang Z, Hu Y, Li B. Vitamin E-based prodrug self-delivery for nanoformulated irinotecan with synergistic antitumor therapeutics. *Int J Pharm*. 2020;15(577):119049. doi:10.1016/j.ijpharm.2020.119049
11. Luo C, Sun J, Sun B, He Z. Prodrug-based nanoparticulate drug delivery strategies for cancer therapy. *Trends Pharmacol Sci*. 2014;35(11):556–566. doi:10.1016/j.tips.2014.09.008
12. Ma ZY, Wang DB, Song XQ, et al. Chlorambucil-conjugated platinum(IV) prodrugs to treat triple-negative breast cancer in vitro and in vivo. *Eur J Med Chem*. 2018;5(157):1292–1299. doi:10.1016/j.ejmech.2018.08.065
13. Burke PJ, Koch TH. Design, synthesis, and biological evaluation of doxorubicin-formaldehyde conjugates targeted to breast cancer cells. *J Med Chem*. 2004;47(5):1193–1206. doi:10.1021/jm030352r
14. Nan Y. Lung carcinoma therapy using epidermal growth factor receptor-targeted lipid polymeric nanoparticles co-loaded with cisplatin and doxorubicin. *Oncol Rep*. 2019;42(5):2087–2096.
15. Taratula O, Garbuzenko OB, Chen AM, Minko T. Innovative strategy for treatment of lung cancer: targeted nanotechnology-based inhalation co-delivery of anticancer drugs and siRNA. *J Drug Target*. 2011;19(10):900–914. doi:10.3109/1061186X.2011.622404
16. Xu C, Wang Y, Guo Z, et al. Pulmonary delivery by exploiting doxorubicin and cisplatin co-loaded nanoparticles for metastatic lung cancer therapy. *J Control Release*. 2019;10(295):153–163. doi:10.1016/j.jconrel.2018.12.013
17. MacEwan SR, Callahan DJ, Chilkoti A. Stimulus-responsive macromolecules and nanoparticles for cancer drug delivery. *Nanomedicine*. 2010;5(5):793–806. doi:10.2217/nnm.10.50
18. She W, Luo K, Zhang C, et al. The potential of self-assembled, pH-responsive nanoparticles of mPEGylated peptide dendron-doxorubicin conjugates for cancer therapy. *Biomaterials*. 2013;34(5):1613–1623. doi:10.1016/j.biomaterials.2012.11.007
19. She W, Li N, Luo K, et al. Dendronized heparin-doxorubicin conjugate based nanoparticle as pH-responsive drug delivery system for cancer therapy. *Biomaterials*. 2013;34(9):2252–2264. doi:10.1016/j.biomaterials.2012.12.017
20. Li H, Bian S, Huang Y, Liang J, Fan Y, Zhang X. High drug loading pH-sensitive pullulan-DOX conjugate nanoparticles for hepatic targeting. *J Biomed Mater Res A*. 2014;102(1):150–159. doi:10.1002/jbm.a.34680
21. Lewis AD, Hayes JD, Wolf CR. Glutathione and glutathione-dependent enzymes in ovarian adenocarcinoma cell lines derived from a patient before and after the onset of drug resistance: intrinsic differences and cell cycle effects. *Carcinogenesis*. 1988;9(7):1283–1287. doi:10.1093/carcin/9.7.1283
22. Ling X, Tu J, Wang J, et al. Glutathione-responsive prodrug nanoparticles for effective drug delivery and cancer therapy. *ACS Nano*. 2019;13(1):357–370. doi:10.1021/acsnano.8b06400
23. Zhang R, Ru Y, Gao Y, Li J, Mao S. Layer-by-layer nanoparticles co-loading gemcitabine and platinum (IV) prodrugs for synergistic combination therapy of lung cancer. *Drug Des Devel Ther*. 2017;5(11):2631–2642. doi:10.2147/DDDT.S143047
24. Johnstone TC, Lippard SJ. The effect of ligand lipophilicity on the nanoparticle encapsulation of Pt(IV) prodrugs. *Inorg Chem*. 2013;52(17):9915–9920. doi:10.1021/ic4010642
25. Wang G, Wang Z, Li C, et al. RGD peptide-modified, paclitaxel prodrug-based, dual-drugs loaded, and redox-sensitive lipid-polymer nanoparticles for the enhanced lung cancer therapy. *Biomed Pharmacother*. 2018;106:275–284. doi:10.1016/j.biopha.2018.06.137

26. Yu W, Liu C, Liu Y, Zhang N, Xu W. Mannan-modified solid lipid nanoparticles for targeted gene delivery to alveolar macrophages. *Pharm Res*. 2010;27(8):1584–1596. doi:10.1007/s11095-010-0149-z
27. Baek JS, Cho CW. A multifunctional lipid nanoparticle for co-delivery of paclitaxel and curcumin for targeted delivery and enhanced cytotoxicity in multidrug resistant breast cancer cells. *Oncotarget*. 2017;8 (18):30369–30382. doi:10.18632/oncotarget.16153
28. Gu Y, Yang M, Tang X, et al. Lipid nanoparticles loading triptolide for transdermal delivery: mechanisms of penetration enhancement and transport properties. *J Nanobiotechnology*. 2018;16(1):68.
29. Zhang M, Zhou X, Wang B, et al. Lactosylated gramicidin-based lipid nanoparticles (Lac-GLN) for targeted delivery of anti-miR-155 to hepatocellular carcinoma. *J Control Release*. 2013;168 (3):251–261. doi:10.1016/j.jconrel.2013.03.020
30. Li M, Tang Z, Lv S, et al. Cisplatin crosslinked pH-sensitive nanoparticles for efficient delivery of doxorubicin. *Biomaterials*. 2014;35 (12):3851–3864. doi:10.1016/j.biomaterials.2014.01.018
31. Xu Z, Liu S, Kang Y, Wang M. Glutathione- and pH-responsive nonporous silica prodrug nanoparticles for controlled release and cancer therapy. *Nanoscale*. 2015;7(13):5859–5868. doi:10.1039/C5NR00297D
32. Gao DY, TsT L, Sung YC, et al. CXCR4-targeted lipid-coated PLGA nanoparticles deliver sorafenib and overcome acquired drug resistance in liver cancer. *Biomaterials*. 2015;67:194–203. doi:10.1016/j.biomaterials.2015.07.035
33. Cai L, Xu G, Shi C, Guo D, Wang X, Luo J. Telodendrimer nanocarrier for co-delivery of paclitaxel and cisplatin: A synergistic combination nanotherapy for ovarian cancer treatment. *Biomaterials*. 2015;37:456–468. doi:10.1016/j.biomaterials.2014.10.044
34. Ni XL, Chen LX, Zhang H, et al. In vitro and in vivo antitumor effect of gefitinib nanoparticles on human lung cancer. *Drug Deliv*. 2017;24 (1):1501–1512. doi:10.1080/10717544.2017.1384862
35. Li F, Mei H, Gao Y, et al. Co-delivery of oxygen and erlotinib by aptamer-modified liposomal complexes to reverse hypoxia-induced drug resistance in lung cancer. *Biomaterials*. 2017;145:56–71. doi:10.1016/j.biomaterials.2017.08.030
36. Whang CH, Yoo E, Hur SK, Kim KS, Kim D, Jo S. A highly GSH-sensitive SN-38 prodrug with an "OFF-to-ON" fluorescence switch as a bifunctional anticancer agent. *Chem Commun*. 2018;54 (65):9031–9034. doi:10.1039/C8CC05010D
37. Luo CQ, Zhou YX, Zhou TJ, et al. Reactive oxygen species-responsive nanoprodrug with quinone methides-mediated GSH depletion for improved chlorambucil breast cancers therapy. *J Control Release*. 2018;28(274):56–68. doi:10.1016/j.jconrel.2018.01.034
38. Zhang Q, Zhang L, Li Z, Xie X, Gao X, Xu X. Inducing controlled release and increased tumor-targeted delivery of chlorambucil via albumin/liposome hybrid nanoparticles. *AAPS PharmSciTech*. 2017;18(8):2977–2986. doi:10.1208/s12249-017-0782-5
39. Chen K, Cai H, Zhang H, et al. Stimuli-responsive polymer-doxorubicin conjugate: antitumor mechanism and potential as nano-prodrug. *Acta Biomater*. 2019;15(84):339–355.
40. Hao DL, Xie R, De GJ, et al. pH-responsive artesunate polymer prodrugs with enhanced ablation effect on rodent xenograft colon cancer. *Int J Nanomedicine*. 2020;16(15):1771–1786. doi:10.2147/IJN.S242032
41. Zhong H, Mu J, Du Y, et al. Acid-triggered release of native gemcitabine conjugated in polyketal nanoparticles for enhanced anticancer therapy. *Biomacromolecules*. 2020;21(2):803–814. doi:10.1021/acs.biomac.9b01493
42. Wang J, Wen Y, Zheng L, et al. Characterization of chemical profiles of pH-sensitive cleavable D-gluconhydroximo-1, 5-lactam hydrolysates by LC-MS: A potential agent for promoting tumor-targeted drug delivery. *J Pharm Biomed Anal*. 2020;185:113244. doi:10.1016/j.jpba.2020.113244
43. Hadipour Moghaddam SP, Yazdimamaghani M, Ghandehari H. Glutathione-sensitive hollow mesoporous silica nanoparticles for controlled drug delivery. *J Control Release*. 2018;28(282):62–75.
44. Wang K, Guo C, Zou S, et al. Synthesis, characterization and in vitro/in vivo evaluation of novel reduction-sensitive hybrid nano-echinus-like nanomedicine. *Artif Cells Nanomed Biotechnol*. 2018;46 (sup2):659–667. doi:10.1080/21691401.2018.1466147
45. Rezaei S, Kashanian S, Bahrami Y, Cruz LJ, Motiei M. Redox-sensitive and hyaluronic acid-functionalized nanoparticles for improving breast cancer treatment by cytoplasmic 17α-methyltestosterone delivery. *Molecules*. 2020;25:5. doi:10.3390/molecules25051181
46. Kim H, Sehgal D, Kucaba TA, Ferguson DM, Griffith TS, Panyam J. Acidic pH-responsive polymer nanoparticles as a TLR7/8 agonist delivery platform for cancer immunotherapy. *Nanoscale*. 2018;10 (44):20851–20862. doi:10.1039/C8NR07201A
47. Poudel K, Gautam M, Maharjan S, et al. Dual stimuli-responsive ursolic acid-embedded nanophytoliposome for targeted antitumor therapy. *Int J Pharm*. 2020;13(582):119330. doi:10.1016/j.ijpharm.2020.119330
48. Oladipo AO, Nkambule TTI, Mamba BB, Msagati TAM. The stimuli-responsive properties of doxorubicin adsorbed onto bimetallic Au@Pd nanodendrites and its potential application as drug delivery platform. *Mater Sci Eng C Mater Biol Appl*. 2020;110:110696. doi:10.1016/j.msec.2020.110696
49. Hu CM, Zhang L. Nanoparticle-based combination therapy toward overcoming drug resistance in cancer. *Biochem Pharmacol*. 2012;83 (8):1104–1111. doi:10.1016/j.bcp.2012.01.008
50. Greco F, Vicent MJ. Combination therapy: opportunities and challenges for polymer-drug conjugates as anticancer nanomedicines. *Adv Drug Deliv Rev*. 2009;61(13):1203–1213. doi:10.1016/j.addr.2009.05.006
51. Eldar-Boock A, Polyak D, Scomparin A, Satchi-Fainaro R. Nano-sized polymers and liposomes designed to deliver combination therapy for cancer. *Curr Opin Biotechnol*. 2013;24(4):682–689. doi:10.1016/j.copbio.2013.04.014
52. Song Z, Shi Y, Han Q, Dai G. Endothelial growth factor receptor-targeted and reactive oxygen species-responsive lung cancer therapy by docetaxel and resveratrol encapsulated lipid-polymer hybrid nanoparticles. *Biomed Pharmacother*. 2018;105:18–26. doi:10.1016/j.biopha.2018.05.095
53. Chou TC, Talalay P. Quantitative analysis of dose-effect relationships: the combined effects of multiple drugs or enzyme inhibitors. *Adv Enzyme Regul*. 1984;22:27–55. doi:10.1016/0065-2571(84)90007-4
54. Kalyane D, Raval N, Maheshwari R, Tambe V, Kalia K, Tekade RK. Employment of enhanced permeability and retention effect (EPR): nanoparticle-based precision tools for targeting of therapeutic and diagnostic agent in cancer. *Mater Sci Eng C Mater Biol Appl*. 2019;98:1252–1276. doi:10.1016/j.msec.2019.01.066
55. Xu Y, Wu H, Huang J, et al. Probing and enhancing ligand-mediated active targeting of tumors using sub-5 nm ultrafine iron oxide nanoparticles. *Theranostics*. 2020;10(6):2479–2494. doi:10.7150/thno.39560
56. Hong Y, Che S, Hui B, et al. Lung cancer therapy using doxorubicin and curcumin combination: targeted prodrug based, pH sensitive nanomedicine. *Biomed Pharmacother*. 2019;112:108614. doi:10.1016/j.biopha.2019.108614
57. Li S, Wang L, Li N, Liu Y, Su H. Combination lung cancer chemotherapy: design of a pH-sensitive transferrin-PEG-Hz-lipid conjugate for the co-delivery of docetaxel and baicalin. *Biomed Pharmacother*. 2017;95:548–555. doi:10.1016/j.biopha.2017.08.090
58. Bian Y, Guo D. Targeted therapy for hepatocellular carcinoma: co-delivery of sorafenib and curcumin using lactosylated ph-responsive nanoparticles. *Drug Des Devel Ther*. 2020;18 (14):647–659. doi:10.2147/DDDT.S238955